PET-COMPTON system. Comparative evaluation with PET system using Monte Carlo simulation

Angelina Díaz García[1], Juan A. Rubio Rodríguez[2], Jose M. Pérez Morales[2], Pedro Arce Dubois[2], Oscar Vela Morales[2], Eduardo Arista Romeu[1], Carlos Willmott Zappacosta[2], Yamiel Abreu Alfonso[1], Antonio Leyva Fabelo[1], Ibrahin Piñera Hernández[1], Lourdes Bolaños Pérez[1]

[1]Centro de Aplicaciones Tecnológicas y Desarrollo Nuclear (CEADEN). Calle 20 Nº 502 esq. a 5ta Ave. Miramar. La Habana, Cuba

[2]Centro de Investigaciones Energéticas, Medioambientales y Tecnológicas (CIEMAT), España

angelina@ceaden.edu.cu

Abstract

Positron Emission Tomography (PET) in small animals has actually achieved spatial resolution round about 1 mm and currently there are under study different approaches to improve this spatial resolution. One of them combines PET technology with Compton cameras. This paper presents the idea of the so called "PET-Compton" systems and has included comparative evaluation of spatial resolution and global efficiency in both PET and PET-Compton system by means of Monte Carlo simulations using Geant4 code. Simulation was done on a PET-Compton system made-up of LYSO-LuYAP scintillating detectors of particular small animal PET scanner named "Clear-PET" and for Compton detectors based on CdZnTe semiconductor. A group of radionuclides that emits a positron (e^+) and γ quantum almost simultaneously and fulfills some selection criteria for their possible use in PET-Compton systems for medical and biological applications were studied under simulation conditions. By means of analytical reconstruction using SSRB (Single Slide Rebinning) method were obtained superior spatial resolution in PET-Compton system for all tested radionuclides (reaching sub-millimeter values of for ^{22}Na source). However this analysis done by simulation have shown limited global efficiency values in "PET-Compton" system (in the order of 10^{-5}-10^{-6} %) instead of values around $5{\cdot}10^{-1}$ % that have been achieved in PET system.

Key words: *compton effect, computerized simulation, Monte Carlo method, positron computed tomography, spatial resolution, G codes*

Sistema PET-COMPTON. Evaluación comparativa con el sistema PET usando la simulación por Monte Carlo

Resumen

En la actualidad la tomografía por emisión de positrones en pequeños animales ha alcanzado valores de resolución espacial cercanos a 1mm y en estos momentos se encuentran bajo estudio diferentes aproximaciones para mejorar dicha resolución espacial. Una de ellas combina la tecnología PET con las cámaras Compton. Este trabajo presenta la idea del denominado Sistema "PET-Compton" e incluye una evaluación comparativa de la resolución espacial y la eficiencia global de los sistemas PET y PET-Compton por medio de la simulación por Monte Carlo utilizando el código Geant4. La simulación fue realizada en un sistema PET-Compton compuesto por detectores centellantes de LYSO-LUYAP de un específico y pequeño escáner PET denominado "Clear-PET" y para detectores Compton en base al semiconductor CdZnTe. Se estudiaron bajo las condiciones de simulación un grupo de radionúclidos que emiten un positrón (e+) y un cuanto gamma casi simultáneamente y cumplen ciertos criterios de selección para su posible utilización en aplicaciones médicas y biomédicas de los sistemas PET-Compton. Por medio de la reconstrucción analítica, empleando el método de reordenamiento de cortes simples (SSRB) se obtuvo una resolución espacial superior para el sistema PET-Compton en todos los radionúclidos de prueba, que alcanzó valores por debajo del milímetro para la fuente de ^{22}Na. Sin embargo, el análisis realizado por medio de la simulación demostró valores limitados de eficiencia global para el sistema PET-Compton (del orden de 10^{-5}-10^{-6}) en contraposición a los valores cercanos a $5{\cdot}10^{-1}$ que se alcanzaron para el sistema PET.

Palabras clave: *efecto compton, simulación computarizada, método de Monte Carlo, tomografía computarizada con positrón, resolución espacial, código G*

Introduction

In order to improve spatial resolution in medical imaging systems preserving its sensitivity, it was considered the possibility of modifying PET scanner in a way that it will be capable a to detect not only two γ quanta from the annihilation of a e+ in coincidence, but also at least one additional γ quantum [1]. If it is possibly to determine the direction of γ quantum that has not come from positron annihilation just one point in the space could be obtained. Moreover, knowledge of the direction of non-positron annihilation generated γ quantum may be relevant for the reconstruction process presumably improving PET's spatial resolution. The aim of this work is to assess, via Monte Carlo simulation, the possibility of obtaining better spatial resolution than that which actually characterizes small animals PET scanners (close to 1 mm) by means of more precise location of the radionuclide emission point and at the same time simplifying the reconstruction process. Technology setup that supports this idea is a combination of two imaging techniques that benefit from the superiority of electronic collimation in terms of better sensitivity: Positron Emission Tomography [2] and a detection system that uses Compton scattering (Compton cameras) [3]. Both systems will be used as a single imaging system, hereinafter referred to as "PET-Compton".

"PET-Compton": PET + Compton

The PET operation principle is based on the detection in coincidence of two γ quanta of 511 keV emitted simultaneously in the opposite directions (at angle 180°), because of the annihilation of e+ when it interact with the electrons of the medium. You can then locate the positron-emitting tracer at some point on the line joining the detectors that record these simultaneous events. The line is called line of response (LoR). It is important to emphasize the necessity for accumulating a large number of LoRs to know more accurately the emitting source position using image reconstruction algorithms.

Imaging systems using the Compton scattering can also determine the position and the source activity. Events can be selected by energy through the sum of the energies deposited in two detectors placed at some distance in the γ-emitting radionuclide field of view. A first detector can measure the kinetic energy deposited by the incident γ quantum E_{γ_1}, its position and interaction time. A resulted γ quantum suffers Compton scattering and hits second detector where its energy E_{γ_2} is absorbed and the time of interaction and position of incidence are recorded. Having time information from both detectors coincidence is registered. Measurements of the position of interaction in each detector determine the direction of scattered γ quantum and having the magnitude of the energy deposited in the first detector the scattering angle is calculated using a formula from Compton kinematics.

$$E_{\gamma_2} = \frac{E_{\gamma_1}}{1 + \frac{E_{\gamma_1}}{m_e c^2}(1 - \cos\theta)} \quad (1)$$

For each event the emission is confined to the surface of a known cone angle (θ), whose apex is determined by the interaction point in the first detector and its axis is defined by the line joining points of interaction in both detectors. The sum of the kinetic energy of the electron and the scattered γ quantum is equal to the incident γ quantum energy. The surface of each cone is a measure of the location of the activity and is obtained through online registration. Three-dimensional distribution of activity is obtained by reconstruction from a large number of cones using appropriate algorithms.

Both PET and Compton systems allow reaching more sensitivity than mechanically collimated Single Photon Emission Tomography systems, but still have limitations to achieve sub millimeter spatial resolution. Also, the complex process of image reconstruction requires a large number of lines of response (LoRs) in the case of PET and cone of response (CoRs) in Compton scattering.

LoR-PET and CoR-Compton intersection

As explained above the idea is to add a Compton imaging detector to a PET system with the intention that not only to detect two 511 keV γ quanta in coincidence from the annihilation of positron but at least as well another additional γ quantum with energy close to 1 MeV. The principle of calculating the emission area is based on the estimation of the intersection of the LoR-PET with CoR-Compton as shown in figure 1.

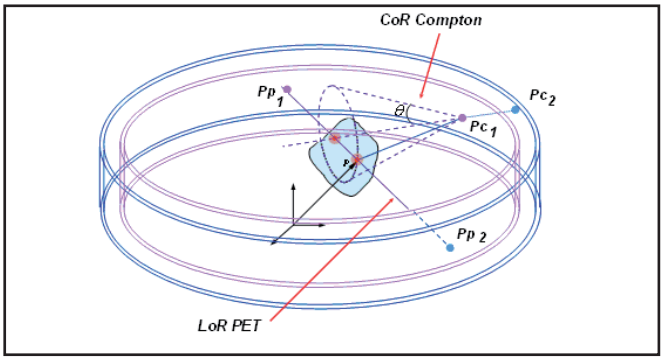

Figure 1. Ilustration of LoR PET and CoR Compton intersection.

The proposal is that using the ε+γ coincidences obtained with specific radionuclides that emit a positron and a γ quantum practically at the same time the location of the emitter source could be measured "in three dimensions".

Simulated "PET-Compton" system consists of two detector rings: smaller inner diameter ring as first (front) Compton scattering detector and an external ring with dual function, second (rear) Compton detector and

PET detector. To achieve optimum performance of this system detectors placed in both rings must have the best possible parameters in terms of spatial, temporal and energy resolution. In theory each ring can separately form LoR-PET but here just the LoRs formed in the outer ring will be considered.

In the absence of errors it is analytically possible to reconstruct the emission point P (figure 2) using the points of interaction in PET (P_{P1}, P_{P2}), the interaction points of the Compton events (P_{C1}, P_{C2}) and the Compton angle θ.

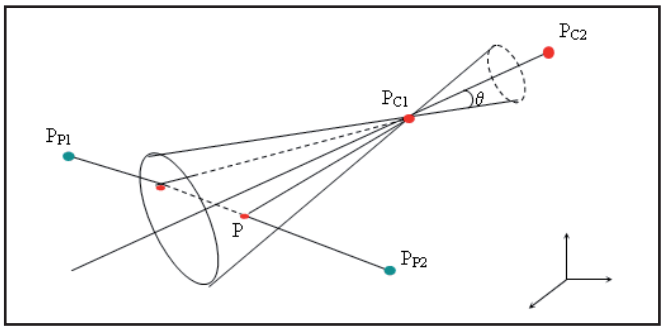

Figure 2. LoR-PET CoR-Compton intersection points.

The searched point P is located in a straight line connecting P_{P1}, P_{P2} and is defined by the parameter λ,

$$\vec{p} = \vec{p}_{P1} + \lambda(\vec{p}_{P2} - \vec{p}_{P1}) \quad (2)$$

Based on geometrical considerations the following expression is obtained:

$$(\vec{p}_{C1} - \vec{p})(\vec{p}_{C2} - \vec{p}_{C1}) = |\vec{p}_{C1} - \vec{p}| \cdot |\vec{p}_{C2} - \vec{p}_{C1}| \cos\theta \quad (3)$$

And substituting (2) in (3):

$$[(\vec{p}_{C1} - \vec{p}_{P1}) - \lambda(\vec{p}_{P2} - \vec{p}_{P1})](\vec{p}_{C2} - \vec{p}_{C1}) = \\ = |\vec{p}_{C1} - \vec{p}| \cdot |\vec{p}_{C2} - \vec{p}_{C1}| \cos\theta \quad (4)$$

This provides:

$$(\vec{p}_{C1} - \vec{p}_{P1})(\vec{p}_{C2} - \vec{p}_{C1}) - \lambda(\vec{p}_{P2} - \vec{p}_{P1})(\vec{p}_{C2} - \vec{p}_{C1}) = \\ = |(\vec{p}_{C1} - \vec{p}_{P1}) - \lambda(\vec{p}_{P2} - \vec{p}_{P1})| \cdot |\vec{p}_{C2} - \vec{p}_{C1}| \cos\theta \quad (5)$$

Introducing the following definitions:

$$(\vec{p}_{C1} - \vec{p}_{P1}) = \vec{v}_1$$
$$(\vec{p}_{C2} - \vec{p}_{C1}) = \vec{v}_2$$
$$(\vec{p}_{P2} - \vec{p}_{P1}) = \vec{v}_3$$
$$\vec{v}_1\vec{v}_2 - \lambda\vec{v}_3\vec{v}_2 = |\vec{v}_1 - \lambda\vec{v}_3| \cdot |\vec{v}_2| \cos\theta$$

Making $\vec{v}_i\vec{v}_j = v_{ij}$ and rising to square both expressions:

$$(v_{12} - \lambda v_{32})^2 = (v_{11} - 2\lambda v_{13} + \lambda^2 v_{33}) v_{22} \cos^2\theta \quad (6)$$

Thus developing the square binomial:

$$(v_{12}^2 - 2\lambda v_{12}v_{32} + \lambda^2 v_{32}^2) = \\ = (v_{11}v_{22} - 2\lambda v_{13}v_{22} + \lambda^2 v_{33}v_{22})\cos^2\theta \Rightarrow$$

$$\lambda^2(v_{32}v_{32} - v_{33}v_{22}\cos^2\theta) + \\ + 2\lambda(-v_{12}v_{32} + v_{13}v_{22}\cos^2\theta) + \\ (v_{12}^2 - v_{11}v_{22}\cos^2\theta) = 0 \quad (7)$$

The above expression is a quadratic equation in λ:

$$a\lambda^2 + b\lambda + c = 0,$$

where

$$\lambda = \frac{-b \pm \sqrt{b^2 - 4ac}}{2a} \quad (8)$$

The solutions to this equation can be:

- Discriminant < 0, there is no real solution, the equation can not be solved and consequently there is not intersection.
- Discriminant = 0, there is one solution and the line is tangential to the cone.
- Discriminant > 0, the line cuts the cone at two points. It is possible to identify the origin of the source through statistics accumulated by the real point source emission.

Described algorithm has been incorporated into the simulation program. Thus the position of the emitting source is directly reconstructed in three dimensions, event by event, allowing further examinations at low count rate and to monitor kinetics of the injected radiopharmaceutical.

Selection of radionuclides

The suggested PET-Compton system assumes the finding of a positron-emitting radionuclide with additional gamma radiation (e+γ). Besides, herein selection was based on two more criteria:

- Physical-nuclear characteristics and production methods.
- Chemical, radiochemical, biological behavior and history of use in biology and medicine of radioactive compounds.

Taking into account also detection properties of the current systems selection has been finally limited

to those radionuclides with the following properties: 1) Energy of e+ decay as low as possible, to avoid uncertainty product of the distance traveled by the e+ before annihilation; 2) non-positron γ quantum have to be issued with high emission rate almost simultaneously with the e+ so that the coincidence time is within the typical detector time resolution which is in the order of 500 psec; 3) γ quantum should preferably be emitted alone to avoid background noise due to spurious signals in the detector and 4) its energy should be greater than energy of γ quanta from the positron annihilation and around 1 MeV, this fact will allow better Compton scattering angular resolution and consequently superior "PET-Compton" spatial resolution at the emission point; 5) The radionuclide half-life has to be short to avoid excessive exposure to radiation but long enough to ensure the quality of the image; 6) Daughter radionuclide must be stable, to prevent further emissions.

From a detailed analysis of the radionuclides that meet these parameters and including also the interest on their current or previous use in biomedical research or medical applications for present simulation of "PET-Compton" system were selected ^{44}Sc [4] , ^{48}V [5] and ^{22}Na [6] radionuclide. ^{22}Na has been included despite its long half-life (2.6 years), which does not allow its use in diagnostic imaging, because is similar in e+ and γ quantum energy emission range to other two selected radionuclides and also ^{22}Na patterns available sources can be used in further experimental studies. Main characteristics of these radioactive sources are shown in table 1and 2.

Table 1. Positron emission characteristic of radionuclides used for Monte Carlo simulation

	e^+ Intensity (%)	e^+ E_{media} (keV)	e^+ E_{max} (keV)	$e^+_{Range\ water}$ (mm)	$e^+_{Dist\ to\ origin}$ (mm)
^{44}Sc	94.34	632.6	1475.3	2.48	1.42
^{48}V	49.9	290.3	694.68	0.85	0.45
^{22}Na	89.84	215.5	545.4	0.542	0.28

Table 2. Gamma emission characteristics of radionuclides used for Monte Carlo simulation

	$\gamma_{Intensity}$ (%)	γ_{Energy} (keV)
^{44}Sc	99.9	1157
^{48}V	100	983.52
	97.5	1312.1
^{22}Na	99.94	1274.53

Materials and methods

Monte Carlo simulation for "PET-Compton" - "ClearPET-CZT" system

For assessing the "PET-Compton" to possibility of obtaining better spatial resolution than PET there were simulated both systems Geant4 code by means of GAMOS framework [7].

For physical processes GAMOS uses the extension to low energies (up to 250 eV) of electromagnetic interactions. In the case of e+ includes the process of annihilation with the electrons of the medium, according to their energy. For electrons and γ quanta takes into account the relevant electromagnetic processes in the energy interval of interest, in this case, Photoelectric, Compton scattering and Raleigh effects for γ quanta and bremsstrahlung and ionization for electrons [8].

Detailed analysis of data was made incorporating to GAMOS the mathematical algorithm of LoR-PET CoR-Compton intersection described in section 2.1. "PET-Compton" results were compared with the results obtained in PET system for the same activity and volume of radiation sources. For reconstruction in PET Single Slice ReBinning (SSRB) analytical method was used.

PET-Compton configuration

Simulated "PET-Compton" system consists in two concentric detector rings. The outer ring is a PET for small animals named "ClearPET" with high spatial resolution (1.25 mm nominal) that uses scintillators detectors of LYSO-LuYAP [9]. This detector ring operates as positron annihilation detector and also as a second Compton scattering detector. The inner ring covers the entire "ClearPET" field of view and it is formed from an array of CdZnTe (CZT) pixelated semiconductor detectors as a front Compton scattering detector. Because it is very important to know as accurate as possible the position of incidence and energy deposited by γ quantum in Compton scattering it has pixels size 300 x 300 μm and high energy resolution (~1,5%). Two implemented in practice "Clear-PET" detector ring diameters (295 and 135 mm) were evaluated. Perspective view of the simulated geometries is shown in figure 3.

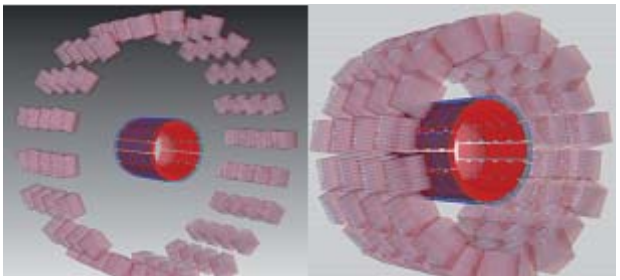

a) $Diameter_{max}$=295 mm b) $Diameter_{min}$=135 mm

Figure 3. PET-Compton perspective view.

Real "ClearPET" parameters obtained from the producer engineering drawings were introduced in the simulation. They are the following:

- Diameter: 295 mm and 135 mm.
- Axial field of view: 110 mm.
- 20 modules (4 rings with 8 x 8 matrixes each coupled to photomultiplier) placed radial.

- Detectors: Arrays of 8 x 8 dual-layer scintillating crystals 2 x 2 x 20 mm^3 each (10 mm thick LYSO: Ce and 10 mm thick LuYAP: Ce), $BaSO_4$ reflector.
- Measurement units: 5120 (8 x 8 x 4 x 20).
- Scintillating crystals units: 10240 (5120 x 2).
- Z axis rotation: 0.1 °, each 2778 events.

Also the axial modules displacement of 7 mm has been introduced in the simulation and only active radiation detectors and $BaSO_4$ reflectors were considered.

CZT detectors parameters used for simulations were the following:

- Ring diameter: 50 mm.
- 5 rings of 15 detectors (10 x 10 x 5 mm^3).
- Detectors - Arrays of 32 x 32 pixels (300 x 300) μm x 5mm.
- Measurement units 75 (5 x 15).
- CZT Units -76 800 pixels (32 x 32 x 15 x 5).

Details of CZT geometry is shown in figure 4 and detection system characteristics introduced in the simulation are shown in table 3.

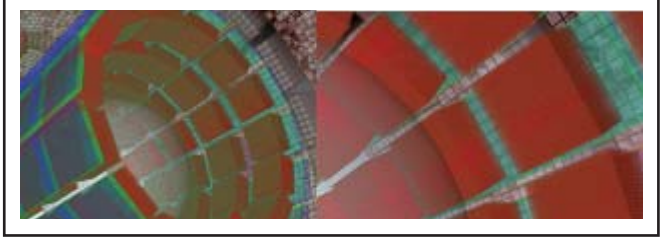

Figure 4. Details of CZT geometry used in PET-Compton simulation.

Table 3. Parameters of the detection system used for simulation

CZT detectors energy resolution (%)	1.5
CZT detectors energy precision (%)	4
ClearPET detectors energy resolution (%)	20
ClearPET detectors energy precision (%)	40
ClearPET and CZT signal measurement time (seg)	10

For the simulation there were used points and spherical (1 mm) ^{44}Sc, ^{48}V and ^{22}Na sources placed in a 4 cm diameter water phantom. In order to visualize the spatial resolution limit simulation was done also for the case of two radioactive sources located at a distance between them slightly larger than positron average range (^{44}Sc-2,5 mm, ^{48}V-1,7 mm, ^{22}Na-0,7 mm). We selected a value of source activity of 10 mCi (370 MBq) and the total number of decays analyzed is $370x10^6$, i.e. the output values correspond to 1 second measurement. The selection of the number of decays analyzed was determined by high consumption of time and computing resources.

Results

Comparison was made for two of the basic parameters that characterize medical imaging systems: spatial resolution (FWHM) and global efficiency. Spatial resolution was determined as the full width half maximum of the Point Spread Function (PSF) peak of radionuclide emission. For "PET-Compton" was obtained by the statistical accumulation of points from LoR-PET CoR-Compton intersection and from the reconstructed events in PET. Global efficiency was determined as the ratio between the number of "PET-Compton" or PET events produced by simulation and the number of total events launched. Figure 5 shows one and two spherical sources placed in water phantom inside the CZT detector ring.

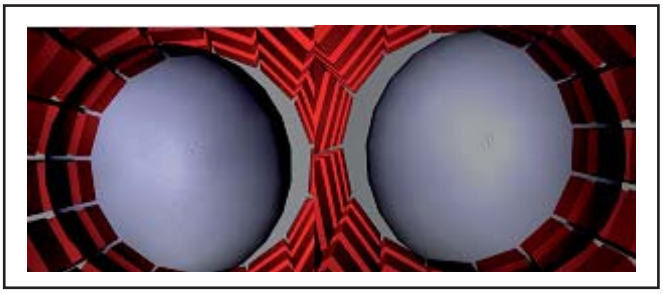

Figure 5. Spherical sources placed in water phantom inside the CZT detector ring obtained by simulation with GAMOS.

Figure 6 shows the magnified view of positron tracking (dashed blue), PET positron annihilation lines (green) and electron scattering (red lines) in water phantom for two point sources of a) ^{44}Sc, b) ^{48}V and c) ^{22}Na. The difference of the positron range for each radionuclide is simply recognized.

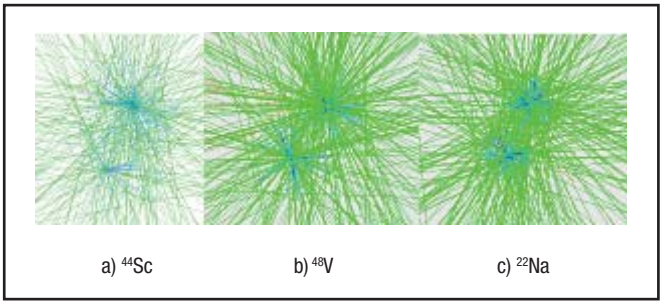

Figure 6. View of the physical processes occurred in two point sources a) ^{44}Sc, b) ^{48}V and c) ^{22}Na.

Spatial resolution (FWHM)

Spatial resolution values were calculated using AMIDE (Medical Image Data Examiner) [10] software, a tool for the analysis of multidimensional medical data. PET and PET-Compton FWHM values for both ClearPET diameters are plotted in figure 7.

For better interpretation the obtained results are shown in table 4 where we can corroborate that in all

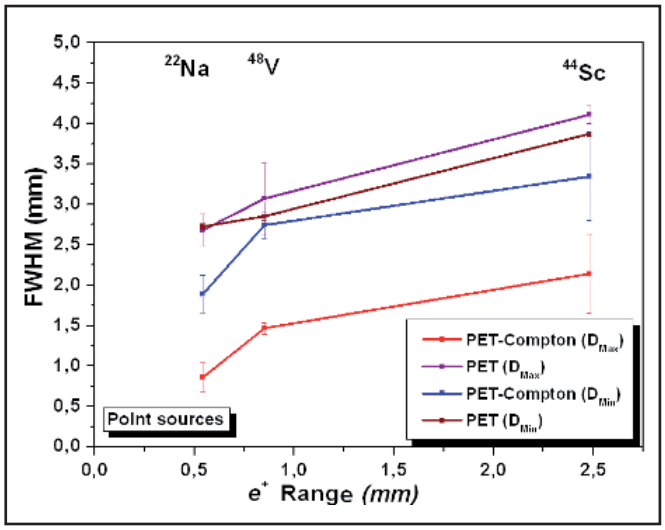

Figure 7. PET-Compton and PET point sources´ spatial resolution for maximum and minimum "ClearPET" diameter.

cases PET-Compton spatial resolution is improved in comparison with spatial resolution obtained for PET only systems using the same radionuclides and simulations parameters.

Table 4. PET-Compton and PET spatial resolution (FWHM) obtained by simulation

	$Diameter_{Max}$ ClearPET		$Diameter_{Min}$ ClearPET	
	PET-Compt	PET	PET-Compt	PET
	FWHM(mm)	FWHM(mm)	FWHM (mm)	FWHM(mm)
^{44}Sc	2.14 +/- 0.49	4.11 +/- 0.1	3.34 +/- 1.5	3.86 +/- 0.03
^{48}V	1.4 +/- 0.08	3.07 +/- 0.4	2.74 +/- 0.16	2.85 +/- 0.05
^{22}Na	0.86 +/- 0.18	2.68 +/- 0.2	1.89 +/- 0.23	2.73 +/- 0.03

Best values of spatial resolution are obtained in PET-Compton settings with greater distance between the ClearPET and CZT rings (maximum "ClearPET" diameter) and it went below 1 mm for ^{22}Na due to its lower e+ range.

In order to see the difference, figure 8 shows the obtained results in AMIDE's visualization screens for PET-Compton (top) and PET (bottom), under the same conditions for simulated ^{44}Sc and ^{48}V radionuclides.

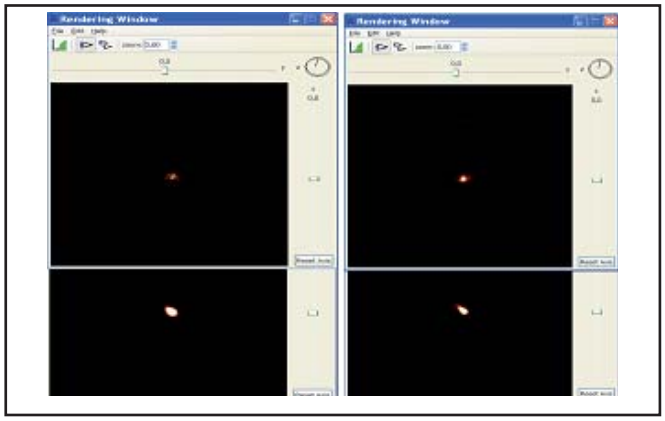

Figure 8. Illustration of ^{44}Sc (left) and ^{48}V (right) point sources in AMIDE's visualization screens. PET-Compton (top), PET (bottom).

In fact for PET-Compton system there is a background of less intense spots corresponding to the second point of intersection LoR-PET CoR-Compton (see equation 8, 2.1 section). However, because its position is random while the accumulation in the real point of emission is high the effect on the screen has been removed rising the lower visualization threshold.

Rendering view of two ^{22}Na point sources in PET-Compton system with better performance (maximum "ClearPET" diameter) placed at 0,7 mm is shown in Figure 9a). For comparison, in Figure 9b) is shown the same view of these two sources in PET system with better resolution (minimum "ClearPET" diameter). Just in the first case two point sources separation can be insinuated.

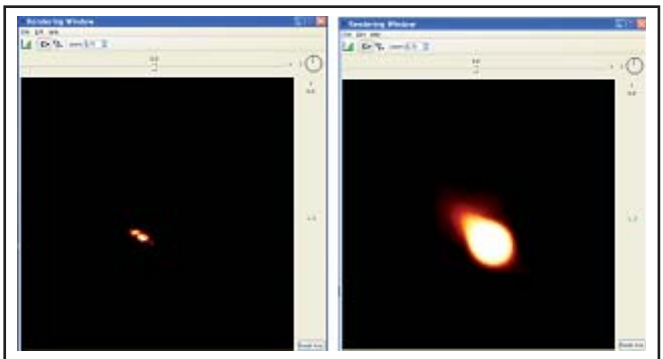

a) PET-Compton ($ClearPET_{Max}$), b) PET ($ClearPET_{Min}$).

Figure 9. AMIDE's rendering view of two ^{22}Na point sources.

FWHM simulation analysis indicates that this "PET-Compton" configuration evidences a possible area of radionuclide emissions much narrower and thus, improved spatial resolution than PET.

Efficiency analysis

In order to estimate global efficiency in "PET-Compton" system and compare it with the efficiency obtained in PET the ratio among simulated events (PET, "PET-Compton") and total launched events under the same simulation conditions was calculated.

Graphics of global system efficiency for the events of each type are shown in Figure 10. For better identification of the results in graphics b) and c) global efficiency values in % of the three radionuclides have been joined in dotted lines (maximum "ClearPET" diameter) and solid lines (minimum "ClearPET"diameter).

The events called $PET\text{-}Compton_{tot}$ are those in which all γ quanta (2γ-PET and 1γ-Compton) had come up from the same radioactive decay and in $PET\text{-}Compton_{valid}$ is added the fact that LoR-PET CoR-Compton intersection point is close to the radionuclide point of emission ($\leq$ 1 mm).

As can be seen efficiency varies over a wide range depending on the type of interaction that occurs within the field of view. Figure 10a) shows PET global efficiency which is about 0.5% (4000-5000 coincidences in 1 million events). Figure 10b) shows

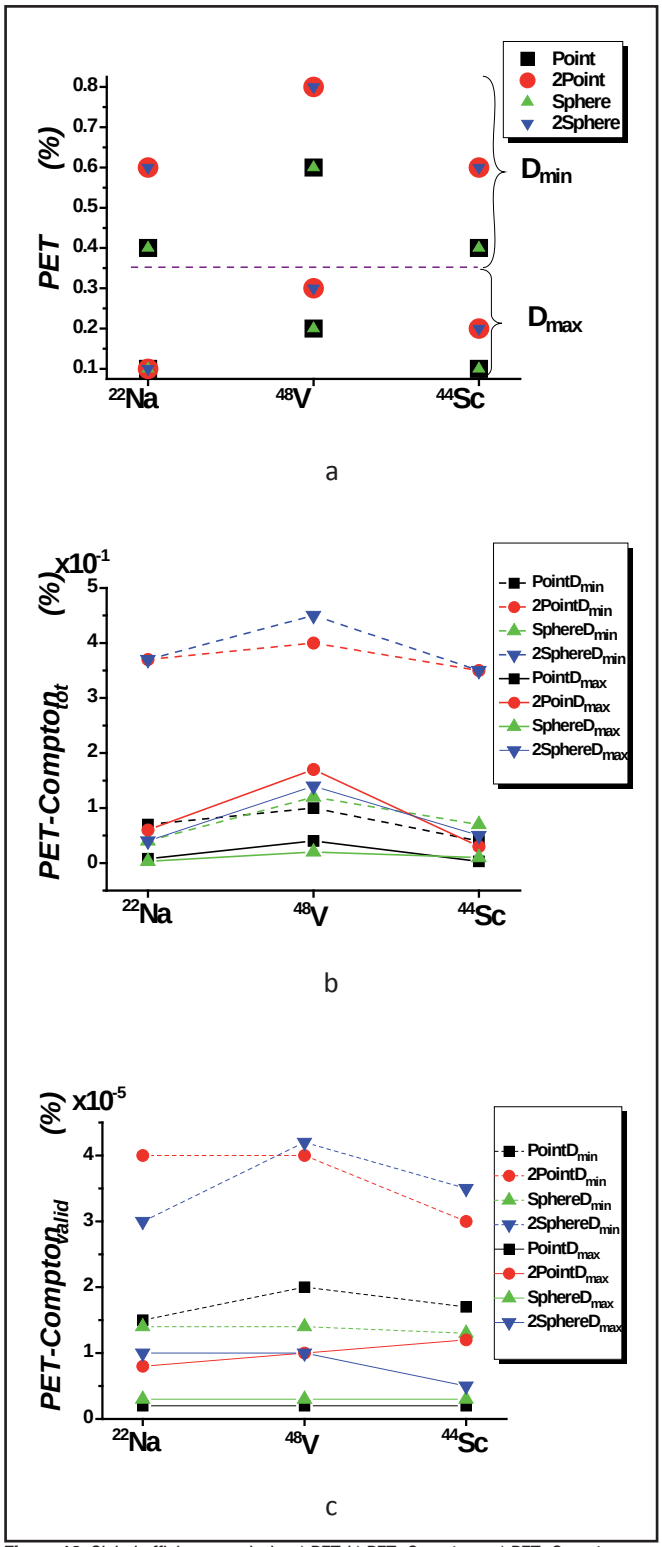

Figure 10. Global efficiency analysis: a) PET, b) PET–Compton$_{tot}$ c) PET–Compton$_{valid}$.

total PET-Compton global efficiency that is of the order of 10^{-1}% for the minimum "ClearPET" diameter and 10^{-2}% for the maximum "ClearPET" diameter. Figure 10c) shows the global efficiency of "valid" PET-Compton events where all γ quanta are from the same decay event and obtained by simulation intersection point are close to the radionuclide emission point. PET-Compton "valid" global efficiency is in the order of 10^{-5}% for the "ClearPET" minimum diameter and 10^{-6}% for the maximum diameter. Besides, it can be observed that in all analyzed cases there is an increased efficiency for ^{48}V radionuclide, because it has two non-positron γ quanta in cascade that have been analyzed as one event. This is acceptable taking into consideration that in current detector systems it is not possible practically to separate this type of events occurring so close in time.

This "PET-Compton" system analysis done by simulation shows limited global efficiency values, particularly when the results are restricted to "valid".

However it is necessary to consider also the fact that due to the large amount of computing resources and time required by the simulation program total number of decays analyzed for each configuration is just 370 x 10^6, hence the output values correspond to 1 second measurement while reasonable measurement time in these techniques are from 15 minutes to 1 hour approximately. The increase in the number of events detected in "valid" PET-Compton, that is possible to achieve increasing simulation time should improve signal to noise ratio and consequently spatial resolution of the system.

Conclusions

Mathematical modeling has demonstrated that the image using "three γ quanta" is expected sharper and could permit more accurate diagnosis. However, the fact that it is necessary to register 4 coincidence events (two corresponding to positron annihilation and two from Compton scattering) significantly limits the global detection efficiency and can affect the spatial resolution for the same statistical data. Thus further development of this method should include the optimization of the factors that could increase global "PET-Compton" efficiency, more specifically, geometric efficiency of the designed system (larger distance between detectors rings and other detection configurations with more efficiency for Compton scattering) is suggested.

Finally would be interesting to note that the simulated system design also allows it use in both, PET and "three γ quanta" mode. They are complementary and the second mode could be used as a higher resolution "lens" when it is required in PET image providing an additional option, certainly for molecular imaging and quite possibly for clinical diagnosis.

Acknowledgements

This work was done under the ITACA* project and we would like to thanks CIEMAT for the financial and technological support.

References

1. HART H. High-Resolution Radioisotopic Imaging System. Patent No. US 4833327. 1989.
2. BAILEY DL, TOWNSEND DW, VALK PE, MAISEY MN. Positron emission tomography: basic sciences. London: Springer-Verlag, 2005.
3. SINGH M. An electronically collimates gamma camera for single photon emission computed tomography. Part I: Theoretical considerations and design criteria. Med. Phys. 1983: 10(4): 421-427.
4. GRIGNON C, et. al. Nuclear Medical Imaging using $\beta+\gamma$ coincidences from 44Sc radio-nuclide with liquid xenon as detetcion medium. Nucl. Instr. and Meth. In Phys. Res. 2007; A571: 142-145.
5. IWATA R, IWAI K, IDO T, KIMURA S. Preparation of no-carrier-added 48 V(IV) and 48V(V) for biological tracer use. J Radioanal. Nucl Chem. 1989; 134(2): 303-309.
6. DAHL LK, SMILAY MG, SILVER L, SPRARAGEN S. Evidence for a Prolonged Biological Half-Life of Na22 in Patients with Hypertension. Circ. Res. 1962; 10: 313-320.
7. ARCE P, RATO P, LAGARES JI. GAMOS an easy and flexible framework for GEANT4 simulations. 2008 Nuclear Science Symposium. Medical Imaging Conference and 16th Room Temperature Semiconductor Detector Workshop. Dresde, Germany, 19-25 October 2008.
8. FIRESTONE RB, EKSTROM L. Table of radioactive isotopes LBNL Isotopes Project-LUNDS Universitet. Version 2.1. January 2004. <http://ie.lbl.gov/toi/>
9. SEMPERE P, ROLDAN E, CHEREUL O, et. al. Raytest ClearPETTM, a new generation of small animal PET scanner. Nucl. Instr.and Meth. 2007; A 571: 498-501.
10. LOENING A, GAMBHIR S. AMIDE: A Free Software Tool for Multimodality Medical Image Analysis. Mol. Imaging. 2003; 2(3): 131-137.

Recibido: 18 de octubre de 2011
Aceptado: 10 de mayo de 2012